Assessment of the Impact of Load Modelling and DSM on Combined Power System Angular and Frequency Stability Using Composite Stability Index

Accepted version of the paper published in IEEE ISGT-Europe 2021

Assessment of the Impact of Load Modelling and DSM on Combined Power System Angular and Frequency Stability Using Composite Stability Index

Mengxuan Wang, *Student Member*, *IEEE*, Jovica V. Milanovic, *Fellow*, *IEEE*
Department of Electrical and Electronic Engineering
The University of Manchester
Manchester, United Kingdom
mengxuan.wang@postgrad.manchester.ac.uk, milanovic@manchester.ac.uk

***Abstract*—With the ever-growing requirement of system stability enhancement, a comprehensive evaluation of overall system stability is coming into research focus to better understand and implement system stability enhancement solutions. This paper proposes a novel Composite Stability Index (CSI) for unified assessment of system frequency and angular stability and illustrates its application considering transient stability, small disturbance stability and frequency stability simultaneously, to assess the impacts of different load models and Demand Side Management (DSM) scenarios on either overall or individual aspects of system stability performance. The results show that the proposed CSI could clearly indicate the distance of operation points to the stability boundary, balance different and even opposite impacts on different stability aspects and quantify the impacts of different load models and DSM deployments on overall system stability performance. The results are illustrated on an equivalent model of four realistic interconnected transmission networks in a DigSilent/PowerFactory simulation environment.**

***Keywords*—Composite Index, Demand Side Management, Load Modelling, Probabilistic Analysis**

I. Introduction

The rapid integration of Renewable Energy Sources (RES) based generation and decommissioning of fossil fuels based synchronous generation has made modern power systems operating closer to the stability boundaries. As a consequence of the reducing capability of traditional methods to maintain system stability, mainly depends on synchronous generators, many novel stability enhancement technologies have been proposed and implemented, such as Flexible AC Transmission System (FACTS), synthetic inertia of wind turbines and Demand Side Management (DSM). The performance and efficiency of these novel technologies and practices are typically determined and quantified considering different aspects of system performance, including different aspects of system stability, separately. Consequently, the conclusions about their overall impact on system performance are often ambiguous and the evaluation of their contribution is not straightforward. There is, therefore, a need for an accurate and efficient assessment of their impact on different, more than one, aspects of system performance simultaneously. Power system stability assessment, which is the focus of this paper, comprising voltage, frequency and angular (small and large disturbance) stability, is a subset of performance criteria that need to be included in this assessment.

The majority of previous assessments of power system stability and the influence of different technologies or operational practices on it, focuses on one or two indices from corresponding stability aspect(s) defined in [1]. In order to improve the accuracy and reliability of system stability evaluation, composite indices have been developed and utilised. The composite index proposed in [2] combines the maximum difference between rotor angles, the maximum difference of rotor speeds, etc. to assess transient stability. Similarly, in [3], the normalised composite transient energy margin is proposed to quantify the severity of the disturbance. On the other hand, there are still very few studies that evaluate multiple stability aspects simultaneously. Centre of inertia based transient stability and frequency stability indices are developed to investigate the distribution of inertia following a disturbance in [4]. Additionally, the impacts of DSM on transient and small disturbance stabilities have been investigated simultaneously in [5] and it has been found that the same DSM action could improve small disturbance stability and deteriorate transient stability at the same time. There is clearly a need to develop an efficient way to evaluate overall system stability performance covering multiple stability aspects and balance sometimes different or even opposite impacts on different stability aspects. This would greatly enhance speed and accuracy of assessment of contribution of different technologies and operational practice, that are rapidly becoming an integral part of modern power system, to overall system stability.

This paper proposes a novel Composite Stability Index (CSI) to assess overall system stability performance, which takes into account the transient stability, small disturbance stability and frequency stability. The proposed CSI can clearly indicate the distance of the system operating point to the stability boundary, recognise system unstable conditions and balance different performances of individual stability aspects. The application of CSI is illustrated on simultaneous assessment of angular and frequency stability of a large, 255-bus, interconnected transmission system comprising four individual realistic transmission networks with 42 equivalent generators. The studies were performed to assess the impact of different load models and DSM actions on the overall system stability (excluding voltage stability). All simulations were performed in a mixed Matlab and DigSilent/PowerFactory environemnt.

II. Composite Stability Index

A. Normalisation of Individual Stability Indices

As mentioned previously, the novel CSI assesses transient stability, small disturbance stability and frequency stability simultaneously. Each stability aspect is evaluated by corresponding, commonly used, stability index, namely Transient Stability Index (TSI) (1) for transient stability, damping of the most critical electromechanical mode (2) for small disturbance stability and frequency nadir (zenith) and Rate of Change of Frequency (RoCoF) (3) for frequency stability.

$$TSI = \frac{360-\delta_{max}}{360+\delta_{max}} \times 100 \qquad (1)$$

$$\lambda = \sigma \pm j\omega \qquad (2)$$

$$ROCOF\ (Hz/s) = \frac{|f_{nadir} - f_{rated}|}{t_{nadir} - t_{disturbance}} \qquad (3)$$

In the above equations, δ_{max} is the maximum rotor angle deviation between any two generators in the system. λ is the eigenvalue of the system state matrix corresponding to the most critical electromechanical mode, σ is the corresponding damping and ω frequency of the mode. Frequency nadir (zenith) is defined as the lowest (highest) frequency value during frequency excursion. f_{nadir} and f_{rated} are frequency nadir (zenith) values and system nominal frequency (50 Hz in this case), respectively. t_{nadir}, and $t_{disturbance}$ are time of frequency nadir (zenith) and disturbance occurrences, respectively.

To maintain system angular stability, TSI needs to be a positive value, while damping needs to be negative. Therefore, 0 has been defined as the stability boundary for both transient and small disturbance stability. In the case of frequency nadir (FN), the limit is defined based on [6] where it is stated that synchronous generators must keep operating for a certain period of time as long as the system frequency is at least 47 Hz, consequently, 47 Hz has been adopted as the stability boundary for FN. Last but not least, [6] also indicates that system components should withstand a RoCoF of up to 1 Hz/s, which has been defined as the stability boundary for RoCoF in this study. Other limits for frequency nadir and RoCoF can be used without any loss of generality.

With the clear definitions of stability boundaries, the distance of each stability index to the corresponding stability boundary is normalised following (4) to (7) for TSI, damping, FN and RoCoF, respectively. The reference values of each stability index have been selected as the largest distance to a corresponding stability boundary observed from a large number of simulations performed.

$$TSI_n = \begin{cases} \frac{TSI-0}{TSI_{Ref}}, & TSI > 0 \\ 0, & TSI \leq 0 \end{cases} \qquad (4)$$

$$\sigma_n = \begin{cases} \frac{0-\sigma}{\sigma_{Ref}}, & \sigma < 0 \\ 0, & \sigma \geq 0 \end{cases} \qquad (5)$$

$$FN_n = \begin{cases} \frac{FN-47}{FN_{Ref}}, & FN > 47\ Hz \\ 0\,, & FN \leq 47\ Hz \end{cases} \qquad (6)$$

$$RoCoF_n = \begin{cases} \frac{1-RoCoF}{RoCoF_{Ref}}\,, & RoCoF < 1\ Hz/s \\ 0\,, & RoCoF \geq 1\ Hz/s \end{cases} \qquad (7)$$

B. Composite Stability Index

The novel CSI is inspired by the equivalent representation of parallel connected impedance. Based on the parallel connected circuit, the structure of the proposed CSI is illustrated in Fig. 1.

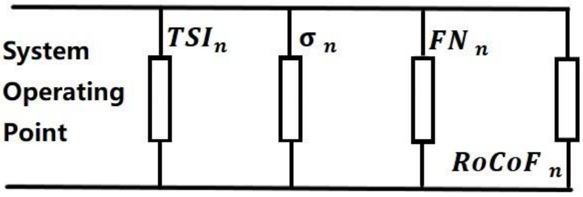

Figure 1: Representation of Structure of CSI

As shown in Fig. 1, due to the fact that all normalised stability indices are derived from the same operating condition, they have been assumed to be four parallel connected impedances. Consequently, the novel CSI is calculated as (8).

$$\frac{1}{CSI} = \frac{1}{4} \times \left(\frac{1}{TSI_n} + \frac{1}{\sigma_n} + \frac{1}{FN_n} + \frac{1}{RoCoF_n}\right) \qquad (8)$$

According to (8), when any of the stability index crosses corresponding stability boundary, CSI equals to 0. Furthermore, $\frac{1}{4}$ is introduced such that CSI equals to 1 when all stability indices are 1, i.e., all stability indices have the largest distance to stability boundary and subsequently, the best stability performance. In normal operational conditions, CSI is a number between 0 and 1, and the higher the CSI value is, the better the overall system performance.

III. System Under Study

A. Overview of the System

The test system adopted in this study is a 255-bus equivalent of four interconnected real transmission networks comprising 42 generators and 178 loads. For reasons of confidentiality, these four interconnected networks are marked as numbers 1 to 4 as shown in Fig. 2.

As can be seen from Fig. 2, the four networks are

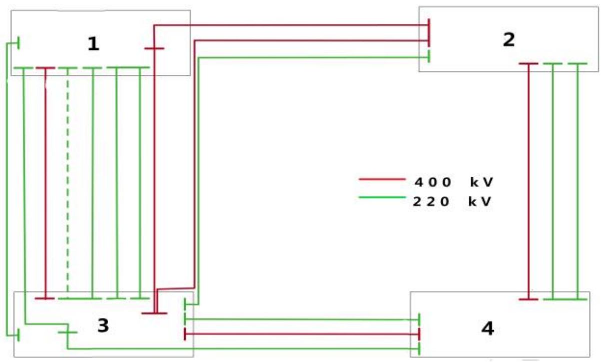

Figure 2: System under Study

interconnected by 17 tie-lines of which 6 are 400 kV lines and 11 are 220 kV lines.

The system daily loading curve is adopted from ENTSO-E report [7], while the normalised system loading curve is obtained by normalising system demand at each hour by the maximum system demand observed throughout the day.

B. Operational Uncertainties and Monte Carlo Simulations

In order to perform Monte Carlo based probabilistic analysis, system operational uncertainties contributed by load demand and wind turbine generation, as well as disturbance uncertainties have been considered and modelled. The details of probability distributions with corresponding modelling parameters are summarised in Table I for all uncertainties under study.

TABLE I: SYSTEM UNCERTAINTIES WITH CORRESPONDING PROBABILITY DISTRIBUTION AND MODELLING PARAMETERS [8-10]

System Uncertainties	**Probability Distributions**	**Modelling Parameters**
Wind Speed and Power Output	Weibull Distribution	$\alpha = 2.2$, $\beta = 11.1$
	Normal Distribution	Mean based on wind speed, $\sigma = 3.33\%$
Load Demand	Normal Distribution	Mean based on load curves, $\sigma = 3.33\%$
Faulted Line	Uniform	N/A
Fault Location	Uniform	N/A
Fault Duration	Normal Distribution	Mean = 5 cycles, σ = 6.67%

It is worth noticing here that wind speeds at different hours throughout the day are modelled following Weibull distribution, while the wind turbine power outputs at one particular hour (i.e., wind speed) are modelled following normal distribution.

The number of Monte Carlo simulations at each hour is determined according to Monte Carlo stopping rules [11], shown as (9). Where X is the data sample with a size of N, E is the sample mean error, Φ^{-1} represents an inverse Gaussian conditional probability distribution (CDF) [11]. Additionally, $\sigma^2(X)$ and $\bar{X}$ are variance and mean values of the sample.

$$\text{E}=\left[\left\{\Phi^{-1}(1-{}^{\delta}/_{2}) \times \sqrt{{}^{\sigma^2(X)}/_{N}}/\bar{X}\right\}\right] \quad (9)$$

To achieve a 99% confidence level in this study, the necessary number of Monte Carlo simulations for TSI, damping, frequency nadir and RoCoF are 60, 20, 25 and 52, respectively. Accordingly, the number of Monte Carlo simulations at each hour is determined to be 100. Mean values of each stability index obtained from 100 Monte Carlo simulations have been adopted to indicate the corresponding stability performance at that hour. All dynamic simulations are performed in DigSilent/PowerFactory 2020 and probability distributions of relevant parameters are generated in Matlab.

C. DSM Deployment Strategies

The DSM implemented in this study is load shifting. To be more specific, load curtailment is conducted during five peak hours (Hours 17 to 21) to reduce system load demand, while disconnected loads are reconnected to the system during five off-peak hours (Hours 1 to 5) leading to increased system load demand. In total, two DSM scenarios have been considered and investigated. The number of DSM assets and DSM capacities (amount of load curtailment or load reconnection in MW) are summarised in Table II for all DSM scenarios. Locations and capacities of DSM assets are reported by Transmission System Operators (TSO) of local networks.

The normalised system daily loading curves without DSM deployment, with DSM scenario 1 and DSM scenario 2, are illustrated in Fig. 3 as a blue solid line, a red dashed line and a black dotted line, respectively.

TABLE II: NUMBER OF DSM ASSETS AND DSM CAPACITIES IN DIFFERENT DSM SCENARIOS

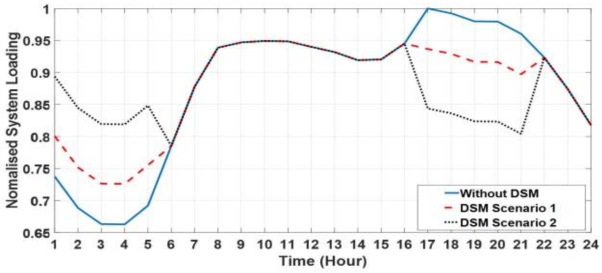

Figure 3: Normalised System Daily Loading Curves with Different DSM Scenarios [7]

	DSM Scenario 1	**DSM Scenario 2**
Name	Current Normal DSM	Future Enlarged DSM
Number of DSM Assets	12	30
Total DSM Capacity	995 MW	1657 MW

D. Study Case

With the purpose of investigating the impacts of different load models and DSM scenarios on overall system stability performance, in total 6 study cases have been developed with different load models and DSM scenarios. All study cases are summarised in Table III. Constant impedance and constant power load models are utilised in this study as according to the results of the international survey reported in [12], they represent the most commonly used load models for system dynamic studies.

TABLE III: STUDY CASES

Study Cases	**Load Model**	**DSM Scenario**
1	Constant Impedance	Without DSM
2	Constant Impedance	DSM Scenario 1
3	Constant Impedance	DSM Scenario 2
4	Constant Power	Without DSM
5	Constant Power	DSM Scenario 1
6	Constant Power	DSM Scenario 2

IV. RESULTS AND ANALYSIS

The disturbances introduced in transient stability assessment and frequency stability assessment are self-clearing three phase short circuit faults and disconnection of the largest power plant, respectively.

A. CSI without DSM Deployment

Focusing on Cases 1 and 4 when the system is operating without DSM, daily overall system stability performances quantified by CSI are illustrated in Fig. 4 as blue solid line and red dashed line for constant impedance load (Case 1) and constant power load (Case 4), respectively. Moreover, the normalised system daily loading curve without DSM has been shown as a black dotted line in Fig. 4.

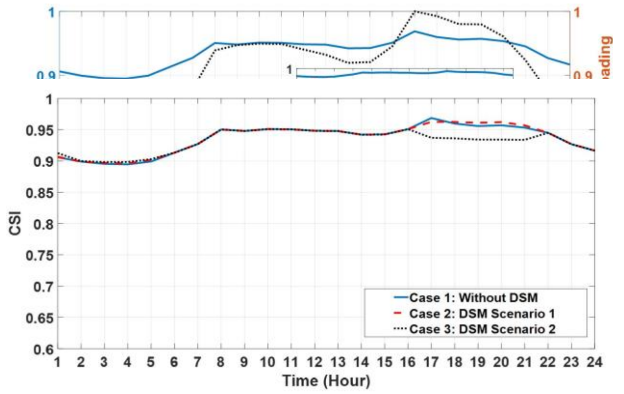

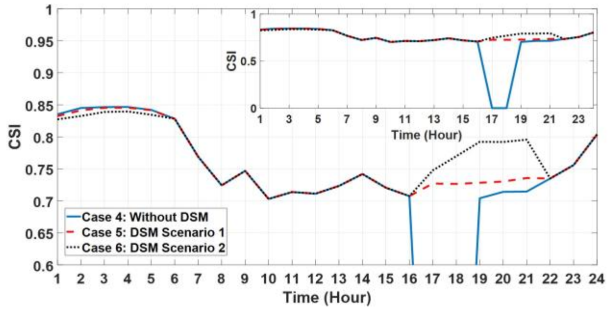

Figure 5: CSI with Different DSM Scenarios for Constant Impedance Load (Left) and Constant Power Load (Right)

It can be seen from Fig. 4 that CSI in Case 1 (constant impedance load) is following the daily loading curve. The overall system stability performance is worse during off-peak hours and it is better during peak hours. In the case of a constant power load model, the trend is the opposite. To be more specific, the overall system stability performance is better during low load periods and it is worse during high load periods. It is worth noticing here that at Hours 17 and 18, the system is unstable as some stability indices exceed the corresponding boundary (CSI=0). Moreover, the red curve is always below the blue curve, indicating that modelling loads as constant power would always result in worse overall stability performance. Last but not the least, due to the fact that the red curve varies over a much larger area than the blue curve, the constant power load model is more sensitive to variation of operating conditions.

In summary, the CSI could clearly indicate a different system stability performance resulting from the use of different load models. Constant power load could be considered as the most critical load model for dynamic studies, due to its high sensitivity to different operational points and potential unstable cases during peak hours.

B. *CSI with Different DSM Scenarios*

The performance of CSI to assess the impacts of DSM on overall stability performance is investigated by comparing Cases 1 to 3 for constant impedance load and Cases 4 to 6 for constant power load. CSI obtained from Cases 1 to 3 and Cases 4 to 6 are shown in the left hand side and the right hand side of Fig 5, respectively.

From the left hand side figure in Fig. 5, it can be noticed that the impact of load curtailment on overall stability performance is much more significant than load reconnection. Load reconnection with constant impedance load is usually beneficial, however the magnitude of impact is minor. The impacts of load curtailment depend on DSM capacity. When the DSM capacity is small (Case 2), load curtailment could either improve or deteriorate overall stability performance. While in Case 3, increased capacity of load curtailment leads to more significant detrimental impacts on overall stability performance.

Regarding the constant power load model, load curtailment during peak hours still shows a more significant effect. Most importantly, load curtailment helps the system to re-gain stability at Hours 17 and 18.

In the case of Cases 4 to 6, load reconnection always results in slightly deteriorated overall stability, while load curtailment always leads to significantly improved overall stability performance. Regardless of the direction of the DSM impacts, both good and bad impacts on overall system stability could be enlarged by increased DSM capacity (Case 6).

Comparing the left hand side figure and the right hand side figure in Fig. 5, the constant power load model is still the most critical load model due to the fact that the same DSM deployment could lead to significant variation of CSI and overall stability performance. Which is reasonable as DSM is actually changing system operation conditions, and the results in the previous section have shown that constant power load model is more sensitive to the change of system operation conditions. Furthermore, the same DSM action could lead to opposite impacts on overall stability performance. This emphasizes the importance of accurate load modelling when assessing the impacts of DSM deployment.

C. *Impacts of DSM on Individual Stability Aspects*

As can be seen from Figs. 4 and 5, the system is overall unstable at Hours 17 and 18, indicating that at least one of the stability aspects considered is unstable at these two hours. From individual normalised stability indices, it can be found that the system is frequency unstable at Hours 17 and 18.

Normalised frequency nadir and normalised RoCoF for both constant impedance and constant power load models are illustrated in Fig. 6 and Fig. 7, respectively.

From Figs. 5 to 7, it can be concluded that frequency stability is dominating the overall system stability performance due to the high similarity between CSI and normalised frequency stability indices. Moreover, it can be seen from Figs. 6 and 7 that different stability indices quantifying the same stability aspect could also indicate very different and even opposite impacts of DSM deployment. For instance, when system loads are modelled as constant power, frequency nadir could always be improved by load curtailment and this beneficial impact could be enlarged by the increased DSM capacity. However, in the case of RoCoF (Fig. 7), load curtailment could lead to either beneficial (Hours 17 and 18) or detrimental (Hours 20 and 21) impacts. Furthermore, increased DSM capacity could also either enlarge (Hours 20 and 21) or reduce (Hours 17 and 18) the existing impacts caused by DSM. These phenomena emphasize the importance of CSI as the CSI could balance different and opposite impacts indicated by different stability indices used for individual assessment of different stability aspects of the system.

V. CONCLUSION

This paper proposes a novel CSI to assess the impacts of load models and DSM deployments on overall system stability performance. The proposed CSI comprises four

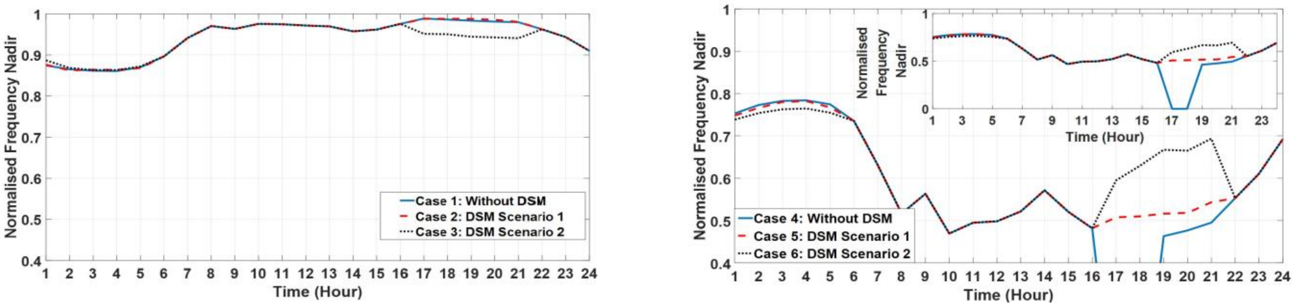

Figure 6: Normalised Frequency Nadir with Different DSM Scenarios for Constant Impedance Load (Left) and Constant Power Load (Right)

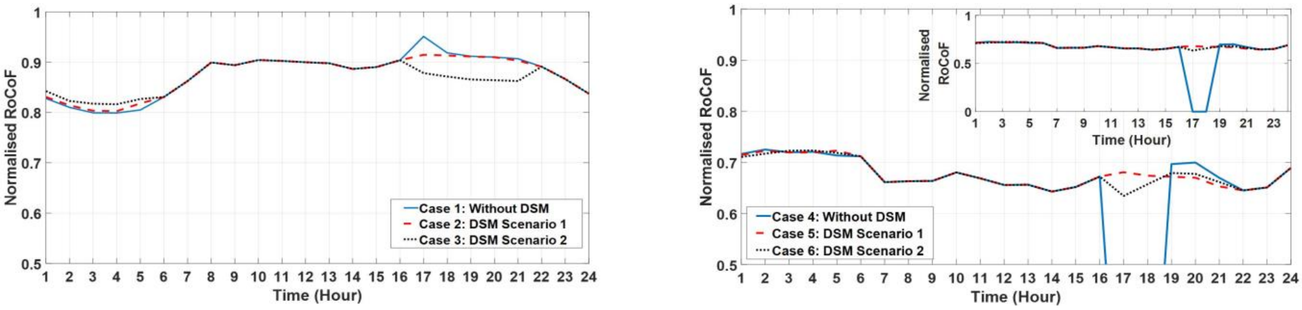

Figure 7: Normalised RoCoF with Different DSM Scenarios for Constant Impedance Load (Left) and Constant Power Load (Right)

normalised stability indices from three different stability aspects, namely transient stability, small disturbance stability and frequency stability. From the results obtained based on two load models (constant impedance and constant power) and three DSM scenarios, it has been proved that the proposed CSI could clearly indicate the distance of system operating points from the stability boundary and balance different and even opposite impacts on individual stability aspects. Furthermore, the proposed CSI could also recognise system unstable situations. Proposed CSI provides a more efficient and comprehensive measure of system stability performance, it could improve the understanding of the impacts of existing and future technologies and stability enhancement solutions on overall stability performance.

To illustrate CSI's applicability, the impacts of DSM with different load models have been assessed. The results indicate that the same DSM action could lead to opposite impacts when system loads are modelled differently. A constant power load model shows, as expected, worse overall stability performance and even yields an unstable system under normal operating conditions. However, DSM deployment is more efficient in the case of constant power load as the overall stability performance alters significantly. All the above-mentioned findings make constant power load the most critical load model when assessing the exact impacts of DSM. Further studies will be performed in the future to incorporate more stability indices into the CSI. Weighting factors of different stability indices will also be considered.

ACKNOWLEDGMENT

The research is supported and partially sponsored by the EU H2020 project CROSSBOW (grant agreement number: 773430) and partly by the Department of Electrical and Electronic Engineering of The University of Manchester. This paper reflects only the authors' views and neither the Agency nor the Commission are responsible for any use that may be made of the information contained therein.

REFERENCES

[1] N. Hatziargyriou, J. V. Milanović, C. Rahmann,V. Ajjarapu, C. Cañizares, I. Erlich, D. Hill, I. Hiskens, I. Kamwa, B. Pal, P. Pourbeik, J. J. Sanchez- Gasca, A. Stanković, T. Van Cutsem, V. Vittal, C. Vournas, "Definition and Classification of Power System Stability – Revisited & Extended", *IEEE Transactions on Power Systems, DOI:10.1109/TPWRS.2020.3041774*.

[2] V. Brandwajn, A. B. R. Kumar, A. Ipakchi, A. Bose and S. D. Kuo, "Severity indices for contingency screening in dynamic security assessment", *IEEE Trans. Power Systems*, vol. 12, no. 3, pp. 1136-1142, August 1997.

[3] C. Fu and A. Bose, "Contingency ranking based on severity indices in dynamic security analysis", *IEEE Trans. Power Systems*, vol. 14, no. 3, pp. 980-986, August 1999.

[4] Y. Wang, H. Silva-Saravia and H. Pulgar-Painemal, "Estimating inertia distribution to enhance power system dynamics", *2017 North American Power Symposium (NAPS)*, USA, 2017.

[5] M. Wang and J. V. Milanovic, "Contribution of advanced demand side management to angular stability of interconnected transmission networks", *IEEE PES Innovative Smart Grid Technologies Conference Europe (ISGT-Europe)*, Romania, 2019.

[6] "Grid Code | Nation Grid ESO". *Nationalgrideso.com*, 2021. [Online]. Available: http://www.nationalgrideso.com/industry-information/codes/grid-code-old?code-documents=. [Accessed: 29/03/2021].

[7] "Monthly Hourly Load Values," entsoe.eu, 2019. [Online]. Available: https://www.entsoe.eu/data/power-stats/hourly load/ [Accessed: 14/10/2019] .

[8] S. Tao, Y. Ruoying, Z. Lingzhi and G. Shan, "Power system probabilistic production simulation containing large-scale wind power and photovoltaic power," in *Proc. IEEE PES Asia-Pacific Power Energy Eng. Conf.*, Dec. 8-11, 2013, pp. 1-6.

[9] R. Preece and J. V. Milanovic, "Tuning of a damping controller for multiterminal VSC-HVDC grids using the probabilistic collocation method," *IEEE Trans. Power Del.*, vol. 29, no. 1, pp. 318-326, Feb. 2014.

[10] T. Guo and J. V. Milanovic, "Probabilistic framework for assessing the accuracy of data mining tool for online prediction of transient stability," *IEEE Trans. Power Systems*, vol. 29, no. 1, pp. 377-385, Jan. 2014.

[11] R. Preece and J. V. Milanovic, "Efficient estimation of the probability of small-disturbance instability of large uncertain power systems", *IEEE Trans. Power Syst.*, vol. 31, no. 2, pp. 1063-1072, Mar. 2015.

[12] CIGRE WG C4.605: "Modelling and aggregation of loads in flexible power networks," Jovica V. Milanovic, (Convenor), (TB 566), ISBN: 978-2-85873-261-6, February 2014.